Morphometric Changes in the Rat Optic Nerve Following Short-term Intermittent Elevations in Intraocular Pressure

Karen M. Joos,[1] *Chun Li,*[2] *and Rebecca M. Sappington*[1]

Purpose. Intraocular pressure (IOP) fluctuations may occur in patients with glaucoma, but how these fluctuations affect axonal populations in the optic nerve and other structures in the eye has been difficult to assess. This study developed a rat model to evaluate the effect of intermittent controlled elevations in IOP on the morphology of the rat optic nerve.

Methods. IOP was transiently elevated for 1 hour on each of 6 days a week over 6 weeks with an adjustable vascular loop around the right topically anesthetized eye of Sprague-Dawley rats. IOP was measured by pneumatonometer before, immediately after, and at the end of 1 hour of treatment with ligature. Globes and optic nerve segments were prepared for histology and morphometry.

Results. Mean baseline IOP of 14.9 ± 1.8 mm Hg increased to 35.3 ± 2.6 mm Hg ($P < 0.001$) during 1-hour treatments and returned to 15.0 ± 2.2 mm Hg ($P = 0.84$) 1 hour after completion. The contralateral untreated eyes had a mean IOP of 14.2 ± 1.9 mm Hg at baseline and 14.6 ± 1.9 mm Hg at the end of treatment. Nerve fiber layer thinning (22%–25%) corresponded with a decrease (7%–10%) in soma number in the ganglion cell layer. Optic nerves displayed axonal degeneration with a modest axon loss of 6% and increased expression of glial acidic fibrillary protein in astrocytes.

Conclusions. Controlled daily 1-hour IOP elevations can be performed with an adjustable vascular loop in rats. After only 6 weeks, intermittent elevations in IOP produce changes in optic nerve consistent with early degeneration reported in chronic models of glaucoma. (*Invest Ophthalmol Vis Sci.* 2010; 51:6431–6440) DOI:10.1167/iovs.10-5212

Chronically elevated intraocular pressure (IOP) is a well-known and well-studied risk factor for glaucomatous optic neuropathy. However, some patients with successful treatment to lower IOP as measured in the clinic, or others treated for normal pressure glaucoma, may have continued glaucomatous progression. This has been hypothesized to be related to transiently elevated IOP perhaps because of medical noncompliance,[1,2] medication troughs,[3] an inversion, Valsalva, or other activities increasing IOP,[4,5] or diurnal fluctuation.[6–11] The detrimental effects of intermittent moderate elevations of IOP on the optic nerve and retina are observed in patients with intermittent uveitic glaucoma[12] or in those with IOP elevations from intermittent steroid use.[13] Furthermore, IOP fluctuations have been suggested to be more common in patients with glaucoma than in subjects without it.[7,14] Greater diurnal IOP fluctuation was recently found in patients treated medically rather than surgically.[15] In a prospective study of 76 patients, those with the largest range of measured IOP had the greatest visual field deterioration over a 2-year period.[16] Similarly, a consistent IOP <18 mm Hg resulted in no visual field deterioration, whereas achieving <18 mm Hg in <50% of visits resulted in visual field deterioration in the Advanced Glaucoma Intervention Study.[17] Therefore, investigating IOP fluctuations in an animal model is clinically relevant.

Current genetic and surgically induced chronically elevated IOP animal models are noted for their variability in IOP measurements among animals.[18–32] However, it is difficult to standardize and explore these fluctuations in a controlled investigation in these models. A well-studied controlled IOP elevation model is used to investigate ocular ischemia.[33–35] However, this rat model represents an extreme global ischemia with IOP elevation beyond the ocular perfusion pressure. In this model, 20 minutes of IOP elevation will produce irreversible ERG changes,[33] and 45 minutes will produce histologic changes.[34] This absolute global ocular ischemia is not representative of the conditions associated with the majority of glaucomas.[35] In addition, this model requires systemic anesthesia and invasive cannulation of the eye, which would be difficult to repeat multiple times in one animal.

The effects of intermittent IOP elevation are not well studied because of lack of control over such fluctuations. A controlled nonsurgical model may offer insights into the earliest changes that could occur in the eye after specified IOP elevation. A model in which IOP can be elevated to partially damage the retinal ganglion cells (RGCs) and their axons and then be restored to normal levels is also desired by investigators to understand which functions are not restored in partially damaged RGCs. This information may suggest potential new therapies to treat injured cells.[36] The purpose of this study was to develop a model in which multiple controlled IOP elevations can be consistently produced in a relatively noninvasive manner and to determine whether basic glaucomatous histologic alterations are detectable after 6 weeks of daily 1-hour IOP elevation.

Methods

Animals and IOP Elevation

All experiments adhered to the ARVO Statement for the Use of Animals in Ophthalmic and Vision Research and were approved by the Institutional Animal Care and Use Committee at Vanderbilt University. Sev-

From the [1]Vanderbilt Eye Institute and the [2]Center for Human Genetic Research, Vanderbilt University, Nashville, Tennessee.

Supported by Fight for Sight Grant-in Aid GA05035 (KMJ); Joseph Ellis Family Glaucoma Research Fund (KMJ); Vanderbilt CTSA voucher from National Center for Research Resources/National Institutes of Health Grant UL1 RR024975 (KMJ); National Institutes of Health Core Grant in Vision Research Grant 2P30EY008126–21; and an unrestricted departmental grant from Research to Prevent Blindness, Inc.

Submitted for publication January 14, 2010; revised May 31, 2010; accepted July 12, 2010.

Disclosure: **K. Joos**, None; **C. Li**, None; **R. Sappington**, None

Corresponding author: Karen Joos, Vanderbilt Eye Institute, 2311 Pierce Avenue, Nashville, TN 37232; karen.joos@vanderbilt.edu.

enteen male retired breeder Sprague-Dawley rats (Harlan Laboratories Inc., Indianapolis, IN) older than 7 months and weighing between 300 and 400 g were used in this study. Animals were fed ad libitum and maintained in climate-controlled rooms with a 12-hour light/12-hour dark cycle. The animals were acclimated to a modified Broome rodent restraint (Fisher Scientific, Pittsburgh, PA; Fig. 1). Topical 0.5% proparacaine hydrochloride was used to anesthetize the rat eyes bilaterally before IOP measurements and before placement of the adjustable ligature around the right eye (Figs. 2A, 2B). The adjustable ligature consists of a 12-cm length of a medium-size vascular loop (Sentinal Loops; Sherwood-Davis and Geck, St. Louis, MO) measuring 2.5 mm wide and 1.3 mm thick, which was inserted within a plastic tubing with 3-mm internal diameter and 1.5-cm length (Figs. 2A, 2B). The loop was placed anterior to the equator of the eye after topical administration of 0.5% proparacaine hydrochloride (Falcon, Fort Worth, TX). A light coating of silicone oil applied to the vascular loop was applied as needed to permit easy adjustment of the tubing and to obtain the desired IOP elevation. Additional topical 0.5% proparacaine hydrochloride was applied to the right eye every 20 minutes while the ligature was in place. One representative animal was anesthetized with ketamine (107 mg/kg; Henry Schein Inc., Palatine, IL), xylazine (27 mg/kg; Henry Schein Inc.), and acepromazine (1.3 mg/kg; Henry Schein Inc.) cocktail intraperitoneally to obtain optic nerve photographs with and without the adjustable ligature in place on the final day.

IOP Measurements

IOP measurements were taken with a precalibrated pneumatonometer[18,37] (Mentor, Norwell, MA). In eight of the rats, IOP was also measured with a second tonometer[19] (Tono-Pen XL; Mentor, Norwell, MA). At each time point, 10 measurements were taken on each eye. The trimmed mean was used in our data analyses. It was calculated by removing the highest and lowest values and averaging over the remaining values. Bilateral measurements were taken before placement of the adjustable ligature. The ligature was applied and adjusted to reach a target IOP of 35 mmHg. IOP measurements were immediately repeated in the right eye and were taken bilaterally before removal of the vascular loop. The ligature was then removed. This procedure was repeated 6 days a week for 6 weeks. IOP measurements were also recorded bilaterally 1 hour after removal of the ligature on the day of perfusion.

Retinal Pathology

Rats were given a lethal dose of anesthesia intraperitoneally and were perfused transcardially with heparinized phosphate-buffered saline followed by 3% paraformaldehyde (catalog no. 158127; Sigma-Aldrich, St. Louis, MO), 0.1% glutaraldehyde (catalog no. 16220; Electron Microscopy Sciences, Hatfield, PA) (vol/vol), and 0.2% saturated picric acid

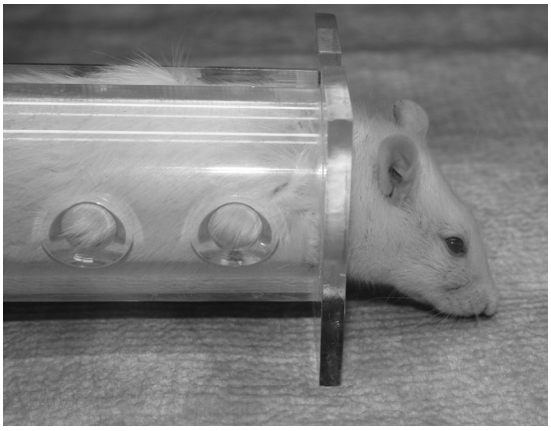

FIGURE 1. The rat is held within a modified Broome restraint during treatment.

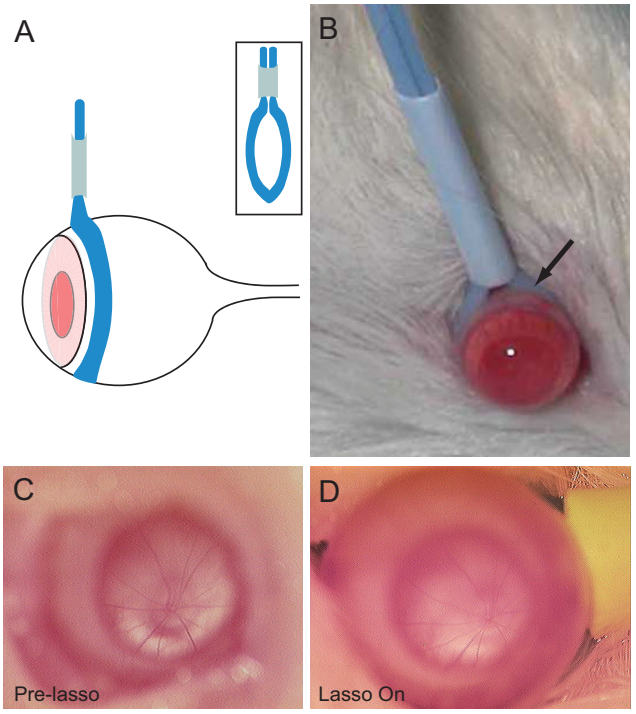

FIGURE 2. Schematic (**A**) and photograph (**B**) of the adjustable vascular loop placed around an eye of a Sprague-Dawley rat posterior to the limbus. Retinal vasculature at the optic disc appears unchanged before (**C**) and while (**D**) the vascular loop is placed around an eye completing 6 weeks of daily elevated IOP.

(catalog no. LC18670; LabChem Inc., Pittsburgh, PA) (vol/vol) in 0.1 M phosphate buffer. After perfusion, the globes and optic nerves were enucleated and separated. The globes were postfixed overnight in the perfusion fixative, dehydrated in graded alcohols and acetone, and embedded in paraffin. Sagittal 7-μm serial sections were stained with hematoxylin (SL90; Statlab, Lewisville, TX) and eosin (C.I. 45380; EMS, Hatfield, PA) for light microscopy.

A masked observer photographed 40× fields (AX70; Olympus, Melville, NY) from serial sections of treated and untreated eyes. Photographs were taken 1 to 2 mm from the optic nerve and in the periphery. The nerve fiber layer (NFL) thickness was measured in three equidistant regions across each photograph using image analysis software (Image Pro Plus 5.1; Media Cybernetics, Silver Spring, MD).[38] Comparisons were made between untreated and treated eyes for both central and peripheral measurements. Cells, including RGCs and displaced amacrine cells, within the ganglion cell layer also were counted within the entire 40× fields with this software.[39] Again, comparisons were made between untreated and treated eyes for both central and peripheral measurements.

Optic Nerve Pathology

The optic nerves 2.5 mm proximal to the globes were removed and fixed in 2% glutaraldehyde (Electron Microscopy Sciences). They were postfixed in 1% osmium tetroxide (catalog no. 19100; Electron Microscopy Sciences) in cacodylate buffer for 1 hour, dehydrated in graded ethanol and acetone, and embedded in Epon (Embed 812; Electron Microscopy Sciences) for evaluation of whole nerve and individual axons. Semithin 1- to 2-μm sections were stained with toluidine blue (Electron Microscopy Sciences) for morphologic evaluation. Ultrathin sections were cut from selected specimens, collected on 200 mesh grids, stained with uranyl acetate (Electron Microscopy Sciences) and lead citrate (Electron Microscopy Sciences), and viewed under a transmission electron microscope (CM-12; Phillips, Hillsboro, OR).

Axon counts were obtained as previously described.[40,41] Briefly, cross-sections of optic nerve were photographed en montage at 100×

magnification (AX70; Olympus, Melville, NY). A previously described set of custom algorithms (courtesy of David Calkins, Vanderbilt University, Nashville, TN) was used to identify and count axons across the entire cross-section as well as measure the entire cross-sectional area of the nerve.[40] This algorithm identifies axons that are defined by the presence of a myelin sheath and counts all these axons in each individual 100× image for the entire montage of the nerve. The resultant data are an actual count of all axons with a myelin sheath that are visible at 100× in the optic nerve cross-section. To control for the previously described variability in axon number between individuals,[42] axon data are represented as the ratio of total axon counts in nerves from treated and untreated fellow eyes. Degenerative profiles were quantified by hand counting of axons with swelling or axonal debris in semithin sections. These counts were performed by a trained, masked observer and are represented as the ratio of degenerative profiles in nerves from treated and untreated fellow eyes. Degenerative changes in the ultrastructure of axons were examined in electron micrographs of nerve cross-sections.

Assessment of Astrocyte Reactivity

Degeneration of the optic nerve also includes activation of glial cells, including astrocytes. Changes in cytoskeletal elements are a hallmark of astrocyte reactivity. To specifically evaluate the reactivity of astrocytes in the optic nerve, we examined changes in immunolabeling of the intermediate filament and astrocyte marker glial fibrillary acidic protein (GFAP) in longitudinal sections of optic nerve. Paraffin sections were deparaffinized and treated for 6 minutes in proteinase K antigen retrieval buffer (S3020; DakoCytomation, Glostrup, Denmark). Sections were then blocked with 5% goat serum and 1% BSA for 30 minutes and subsequently were incubated in primary antibody GFAP (1:1000; Z0334; DakoCytomation) at 4°C overnight. Secondary staining was performed with AlexaFluor 488 F(ab)2 fragment of goat anti-rabbit IgG (H+L) at 1:100 concentration (A11019; Invitrogen, Carlsbad, CA). Controls for immunohistochemistry experiments were conducted with no primary antibody and the appropriate IgG isotype. At least six confocal micrographs (60× magnification) were obtained for each nerve analyzed on an upright confocal microscope equipped with laser scanning fluorescence (blue/green, green/red, red/far-red) and Nomarski-DIC, 3D z-series, and time series (LSM 510; Zeiss, Thornwood, NY) in the Vanderbilt Cell Imaging Core. Changes in immunolabeling intensity were quantified by spectral analysis of fluorescent signal using an image analysis software package (Image Pro Plus; Media Cybernetics, Silver Spring, MD).

Statistical Analysis

IOP Measurements. For each rat and each day, the difference in IOP before and during ligature was calculated. Because there were multiple observations for each rat, the data were not independent. Instead the measurements were averaged at each time point for each individual rat. Within each group, each rat was observed for the same number of days for the time points (before and during the lasso). We calculated the difference for each day for each rat. Then we calculated the average for each rat across the days as the within-subject average and their average across rats as the overall average. Paired *t*-tests were then performed. The analyses were carried out in R (www.r-project.org). Repeated-measures ANOVA was also performed to estimate the fractions of within-rat and between-rat variations for the IOP increase attributed to treatment.

Retinal Pathology. The Mann-Whitney rank sum test was used to compare the thickness of the nerve fiber layer in untreated versus treated retinas. A two-sample, unpaired *t*-test was used to compare the number of cell soma in the ganglion cell layer in untreated versus treated retinas. To determine the appropriate statistical tests, normality (Shapiro-Wilk Normality Test) and variance (Equal Variance Test) of all data were examined before variance analysis. All analyses were conducted in statistical analysis software (SigmaPlot/SigmaStat, version 11.0; Systat, Inc., San Jose, CA). For all analyses, $P \leq 0.05$ was considered statistically significant.

Optic Nerve Pathology. The Wilcoxon signed rank test was performed to compare the numbers of degenerating axons per cross-section between the two eyes. A one-sample *t*-test was performed to compare the ratios of total axons, cross-sectional area, and GFAP intensity in treated and untreated optic nerves to the hypothetical population value of 1.0. Before variance testing, the normality of all data was examined using the Shapiro-Wilk normality test. All analyses were conducted in statistical analysis software (SigmaPlot/SigmaStat, version 11.0; Systat, Inc.). For all analyses, $P \leq 0.05$ was considered statistically significant.

Results

Uniform and Intermittent Elevations in IOP with Adjustable Ligature

IOP was measured 6 days a week over 6 weeks. On each day, the IOP was easily and immediately elevated in the right eye with the adjustable lasso (Figs. 2, 3). All the rats gained

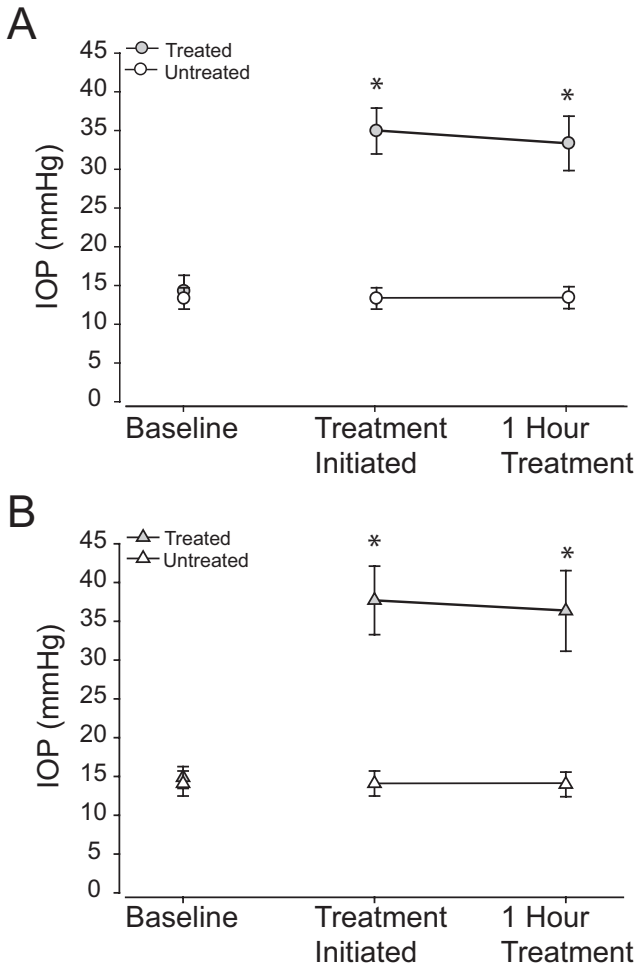

Figure 3. (**A**) Mean (± SD) IOP measurements by pneumatonometer before placement of the vascular loop (baseline), immediately after placement of the vascular loop, and at the end of the 1-hour IOP pressure elevation session in the treated right eye and in the untreated left eye of all rats completing 6 weeks of daily elevated IOP. (**B**) Mean (± SD) IOP measurements by tonometer before placement of the vascular loop, immediately after placement of the vascular loop, and at the end of the 1-hour IOP pressure elevation session in the treated right eye and in the untreated left eye of all rats completing 6 weeks of daily elevated IOP. *Asterisk*: statistical significance. The IOP is elevated immediately after placement in the vascular loop around the eye.

weight and appeared to tolerate the daily transient IOP elevations without evidence of distress. The external appearance of the eyes and adnexa remained normal over the 6 weeks. The number of animals that could be tested at one time was limited by the number of rat restraints available and the number of IOP measurements taken daily per animal. Ophthalmoscopy of the optic nerve before (Fig. 2C) and after placement of the lasso (Fig. 2D) demonstrated continued retinal perfusion.

With the pneumatonometer, the mean baseline IOP in the untreated eye was 14.2 ± 1.9 mm Hg and averaged 14.6 ± 1.9 mm Hg at the end of treatment (Fig. 3A). The mean baseline IOP in the treated eyes was 14.9 ± 1.8 mm Hg (Fig. 3A). During ligature, IOP increased to 35.3 ± 2.6 mm Hg ($P < 0.001$) initially and to 34.4 ± 3.1 mm Hg ($P < 0.001$) at the end of the 1-hour treatments over 6 weeks (Fig. 3A). This was an average increase in IOP of 20.4 mm Hg ($P < 0.001$) with ligature compared to baseline. IOP returned to 15.0 ± 2.2 mm Hg ($P = 0.84$) 1 hour after treatment completion, as measured on the last day.

To confirm the pneumatonometer measurements, IOP was also measured using a second tonometer (Tono-Pen XL; Mentor) in eight of the rats, which yielded measurements consistent with those obtained with the pneumatonometer. The mean baseline IOP in the untreated eyes was 14.1 ± 1.6 mm Hg and averaged 14.0 ± 1.6 mm Hg ($P = 0.14$) at the end of treatment (Fig. 3B). The mean baseline IOP in the treated eyes was 14.9 ± 1.4 mm Hg (Fig. 3B). During ligature, IOP increased to 37.7 ± 4.4 mm Hg ($P < 0.001$) initially and to 36.3 ± 5.2 mm Hg ($P < 0.001$) at the end of the 1-hour treatments over 6 weeks (Fig. 3B). This was an average increase in IOP of 22.8 mm Hg ($P < 0.001$) with ligature compared with baseline. IOP returned to 17.9 ± 0.7 mm Hg ($P = 0.42$) 1 hour after treatment completion, as measured on the last day.

To determine the consistency of IOP elevation over the 1-hour treatment, the difference was calculated between the pressures immediately and 1-hour after the lasso was placed. By pneumatonometer, pressure in the treated eyes decreased by 0.9 ± 0.8 mm Hg over the 1-hour treatment period ($P < 0.001$; Fig. 3A). Untreated eyes revealed an increase of 0.4 ± 0.3 mm Hg over the 1 hour treatment period ($P < 0.001$). Similarly, in eight of the rats with IOP also measured by the second tonometer (Tono-Pen XL; Mentor), pressure in the treated eyes decreased by 1.4 ± 2.0 mm Hg over the 1-hour treatment period ($P < 0.001$; Fig. 3B). Untreated eyes revealed a decrease of 0.1 ± 1.4 mm Hg over the 1-hour treatment period ($P = 0.14$).

Repeated-measures ANOVA estimated the fractions of within-rat and between-rat variations for the IOP increases attributed to treatment. For the second tonometer (Tono-Pen XL; Mentor)–measured rats, the fraction of within-subject variation was 0.9999 and that of between-subject variation was 0.0001. For the pneumatonometer-measured rats, the fractions were 0.997 and 0.003. These results suggest that the across-rat variation was very small compared with the overall variation. Thus, the conclusion from repeated-measures ANOVA was the same as that of the paired *t*-tests. Together, these data suggest that pressure applied to the exterior of the globe by a vascular loop produces controlled elevations in IOP that are highly consistent both within and between animals.

Early Retinal Injury with Intermittent IOP Elevation

The ocular tissues were examined for signs of overt injury or inflammation. After 6 weeks of intermittent IOP elevation, the corneas remained clear. Histology demonstrated that the angles remained open (Figs. 4A, 4B). In addition, no inflammatory cells were noted within the corneal stroma and the anterior chamber angle. The layers of the retina appeared grossly intact without obvious destruction in the treated eye compared with the untreated eye (Figs. 4C–H). No obvious increase in inflammatory cells was present (Figs. 4C–H). A suggestion of increased optic nerve cupping is present in the treated eyes (Figs. 4D, 4F) compared with their respective untreated eyes (Figs. 4C, 4E). Retinal layers were intact in both untreated and treated eyes (Figs. 4G, 4H). No evidence of ischemic injury was present.

To determine whether daily IOP elevations of 1 hour for 6 weeks were sufficient to induce pathology in the ganglion cell and nerve fiber layers of the retina, we measured both the number of cell soma in the ganglion cell layer and the thickness

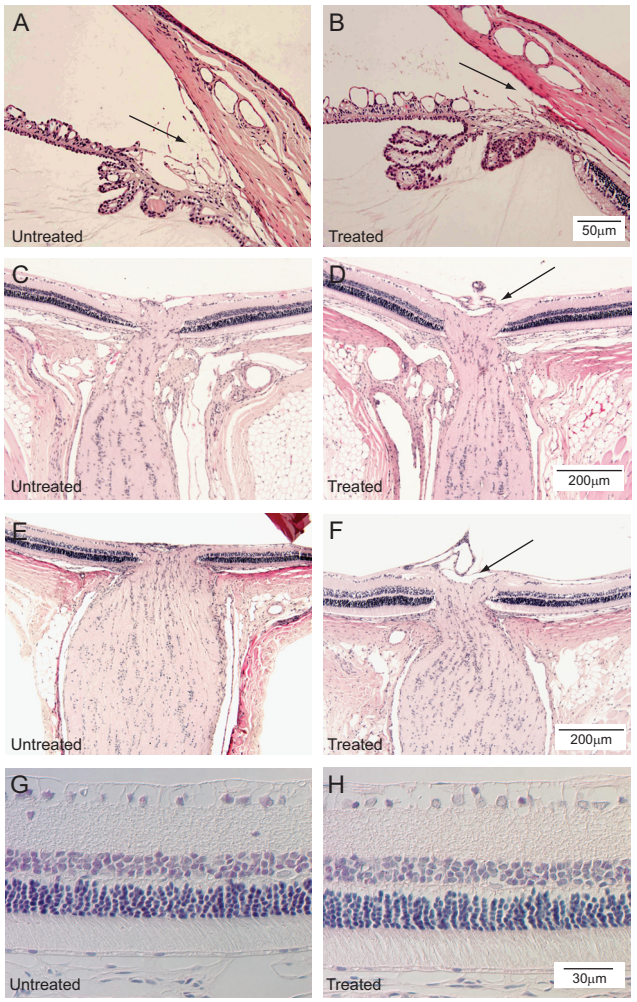

Figure 4. Histologic sections of the anterior chamber angles of one 6-week-treated rat with the untreated eye (**A**) and treated eye (**B**) for comparison (hematoxylin and eosin; scale bar, 50 μm). No evidence of synechiae is present in the angle. Histologic sections of the retina and optic nerves of one 6-week-treated rat with the untreated eye (**C**) and treated eye (**D**) for comparison. Retinal ganglion cells are present in both specimens. No evidence of ischemic injury is present (hematoxylin and eosin; scale bar, 200 μm). A suggestion of increased optic nerve cupping is present in the treated eye (*black arrow*). Histologic sections of the retina of another rat with the untreated eye (**E**) and treated eye (**F**) for comparison demonstrates similar findings (hematoxylin and eosin; scale bar, 200 μm). A suggestion of increased optic nerve cupping is present in the treated eye (*black arrow*). Retinal layers are intact in both untreated (**G**) and treated (**H**) eyes. No evidence of ischemic injury is present (hematoxylin and eosin; scale bar, 30 μm).

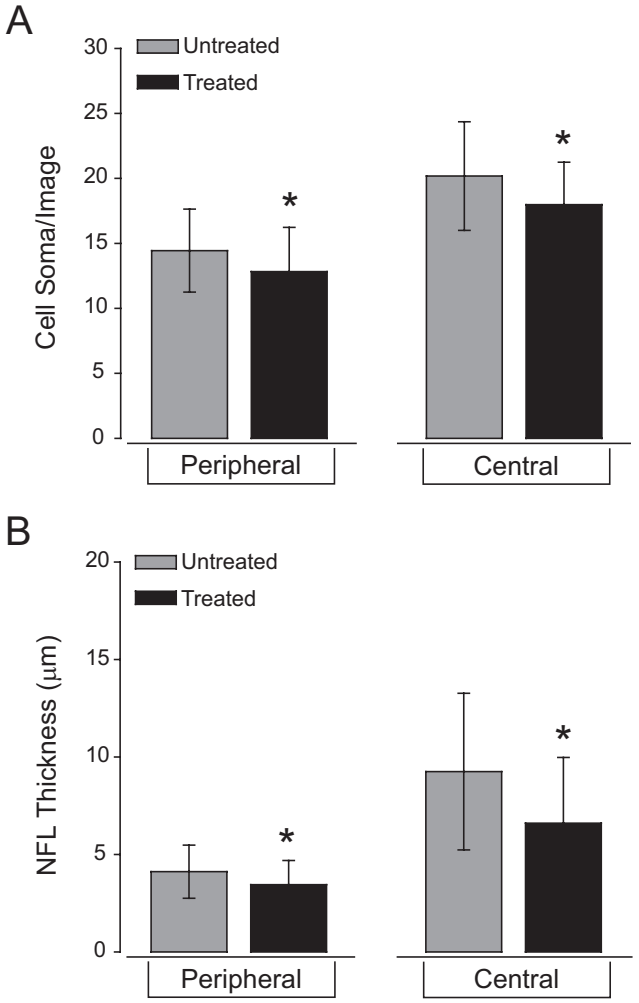

FIGURE 5. Quantification of cell soma number in the ganglion cell layer (**A**) and nerve fiber layer thickness (**B**) in untreated eyes and treated eyes receiving 6 weeks of daily, 1-hour IOP elevations. (**A**) There are significantly fewer cells within the ganglion cell layer in treated eyes than in untreated eyes both near the optic nerve head and in the periphery ($P < 0.01$). (**B**) The retinal nerve fiber layer is significantly thinner in the treated eyes than in the untreated eyes both near the optic nerve head and in the periphery ($P < 0.01$). *Asterisks*: statistical significance.

of the NFL. To account for changes in eccentricity, we quantified cell soma number and NFL thickness in 40× images from the peripheral and the central retina independently. In peripheral retina, the mean number of cell soma per image was 13 ± 3 in treated eyes compared with 14 ± 3 in untreated eyes (Fig. 5A). This difference corresponds to a 7% decrease in cell soma number that is statistically significant ($P = 0.01$; Fig. 5A). Similarly, the mean number of cell soma per image in the central retina also decreased by 10% in treated eyes (18 ± 3) compared with untreated eyes (20 ± 4; $P < 0.01$; Fig. 5A). In accordance with the cell soma data, NFL thickness in the peripheral retina decreased by 25% in treated eyes (3 μm ± 1 μm) compared with untreated eyes (4 μm ± 1 μm; $P < 0.01$; Fig. 5B). In the central retina, NFL thickness also decreased by 22% in treated (7 μm ± 3 μm) versus untreated eyes (9 μm ± 4 μm; $P < 0.01$; Fig. 5B). These data suggest that intermittent IOP elevation over a 6-week period induces slight, but detectable, thinning of the NFL that corresponds with loss of cell soma in the ganglion cell layer of the retina.

Optic Nerve Pathology with Intermittent IOP Elevation

Optic nerve morphology was examined after intermittent elevation of IOP for 6 weeks. Consistent modest and intermittent elevations in IOP (Fig. 3) produced an increase in the incidence of degenerative axon profiles and vacuolization in the extra-axonal space (Figs. 6A–D). By light microscopy, the degenerative profiles were characterized by hypermyelination and enlargement of the axoplasm (Figs. 6C, 6D). The appearances included empty vacuoles, swollen axons with disruption of the neurofilaments, densities with collapsed myelin sheaths, or loosening of the myelin sheath. Electron microscopy revealed that the myelin sheaths associated with these degenerative profiles were significantly disorganized with intermittent areas of collapsed sheath (Fig. 6E). Disruption of neurofilaments was also evident in degenerative profiles with an enlargement of the axoplasmic space (Fig. 6E). Quantification of degenerative profiles revealed that the number of degenerative profiles increased 4.4-fold on average in treated nerves compared with untreated nerves ($P = 0.04$; Fig. 6F). However, there was significant variability in the number of degenerative profiles between animals (Fig. 6F).

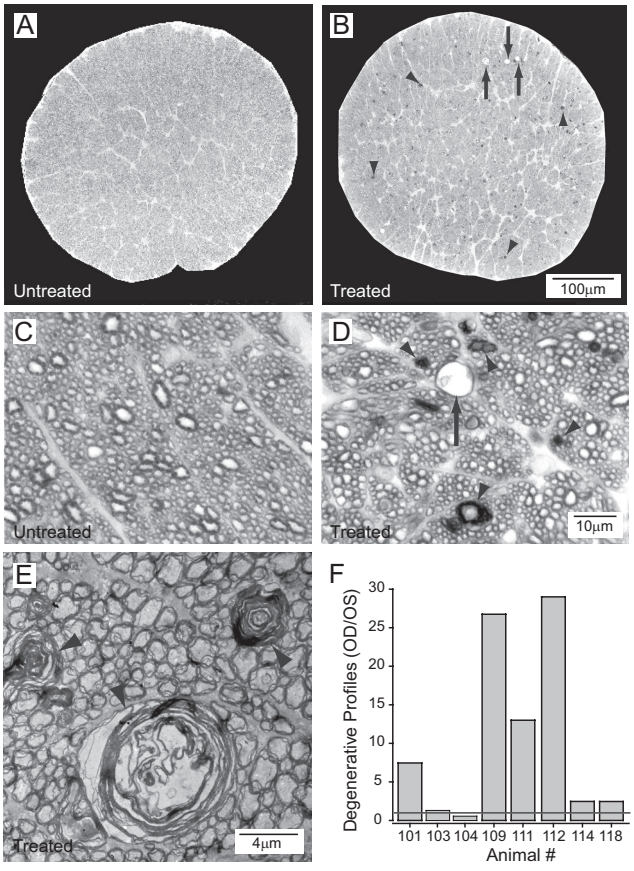

FIGURE 6. Representative semithin rat optic nerve cross-sections (toluidine blue) of an untreated eye (**A**, **C**) and the contralateral 6-week treated eye (**B**, **D**). More alterations of axonal structures are present in the treated side (**B**, **D**) with degenerated axons (*arrowheads*) and vacuoles (*arrows*) compared with structures in the untreated side (**A**, **C**). (**E**) Myelin wrapping abnormalities (*arrowheads*) in the optic nerve are evident in an electron micrograph of a 6-week treated eye. (**F**) More degenerating profiles are observed in optic nerve cross-sections in treated compared with untreated contralateral eyes. Although treatment was uniform, some animals had a greater degenerative response than other individuals.

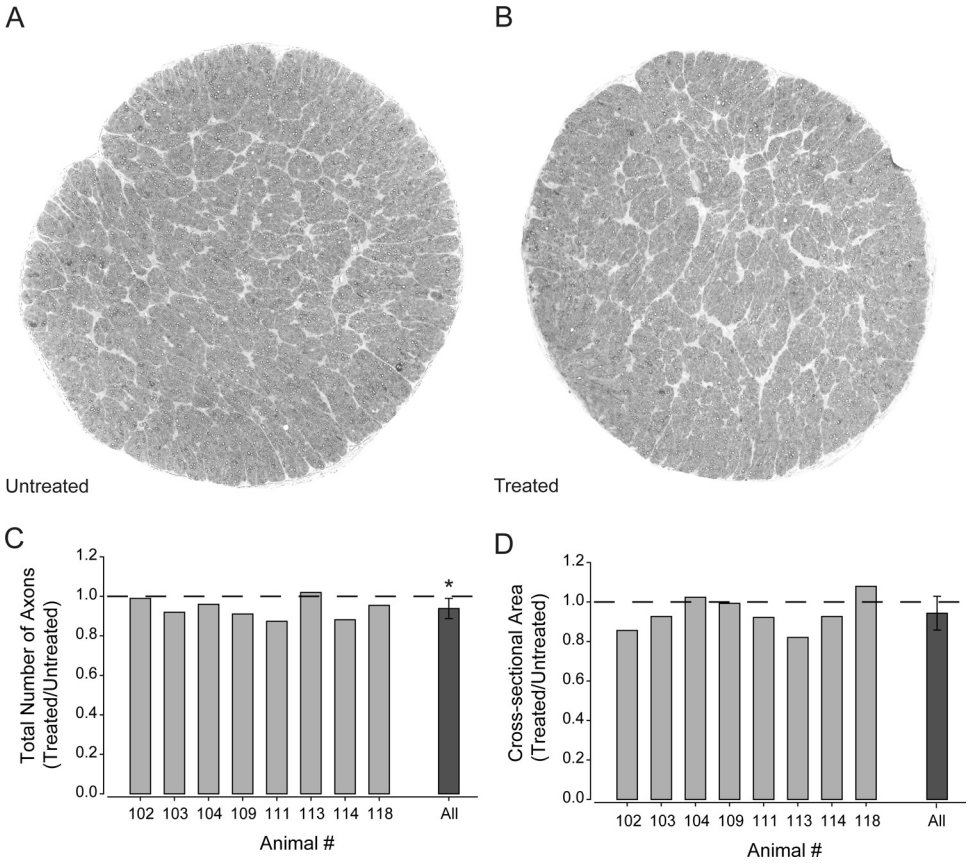

FIGURE 7. Quantification of total axon number and cross-sectional area of optic nerves from untreated eyes and the contralateral 6-week treated eye. (**A**) Representative montage (100×) of optic nerve cross-section from contralateral untreated eye. (**B**) Representative montage (100×) of optic nerve cross-section from treated eye. (**C**) Total number of axons in an entire optic nerve cross-section represented as the ratio of axons in treated versus untreated optic nerves. Graph depicts the ratios for individual animals (*light gray*) and the combined ratio across all animals (*dark gray*). The total number of axons is significantly lower in treated nerves compared with untreated nerves ($P = 0.01$). (**D**) Cross-sectional area of entire optic nerve represented as the ratio of area in treated versus untreated optic nerves. Graph depicts the ratios for individual animals (*light gray*) and the combined ratio across all animals (*dark gray*). The cross-sectional area of the optic nerve did not differ between treated and untreated optic nerves ($P = 0.10$). *Asterisk*: statistical significance.

Measurable Loss of Axons with Intermittent IOP Elevation

To determine whether 6 weeks of intermittent IOP elevation results in measurable loss of axons in the nerve, the total number of axons was quantified in whole cross-sections of optic nerve (Figs. 7A, 7B; see Methods). To account for naturally occurring individual variances in total axon number,[42] the total axon number was evaluated as the ratio of total axons in treated over untreated optic nerves. The average number of axons was 6% lower in treated optic nerves (87,098 ± 12,487) than in untreated nerves (92,919 ± 13,442; Table 1; Fig. 7C). This difference in axon number was diffuse across the nerve rather than concentrated in any one sector (Figs. 7A, 7B). Comparison of changes in the ratio of total axons in treated versus untreated nerves across individual animals revealed that this modest decrease in axon number was consistent between animals and was statistically significant across animals ($P = 0.01$, Fig. 7A). These data suggest that only 1 hour of elevated pressure daily for 6 weeks is sufficient to cause modest loss of RGC axons in the optic nerve. This pressure-induced decrease in axons correlates well with the reduction in NFL thickness and the number of cell soma in the ganglion cell layer noted in Figure 5.

Previous studies suggest that the cross-sectional area of optic nerve can shrink during degeneration caused by chronic elevations in IOP.[43–45] To assess the cross-sectional area with intermittent IOP elevations, the cross-sectional area of the nerve was measured and compared between untreated and treated eyes. Again, the ratio of the treated to untreated optic nerves was examined to account for individual variability.

TABLE 1. Quantification of Optic Nerve Pathology: Cross-Sectional Area, Total Axon Number and Degenerating Axon Counts for Treated and Untreated Nerves from Individual Animals

	Cross-Sectional Area (mm^2)		Axons in Nerve (*n*)		Degenerating Axons per Cross-Section (*n*)	
Rat	**Treated**	**Untreated**	**Treated**	**Untreated**	**Treated**	**Untreated**
102	0.252	0.296	81,504	82,371	82	11
103	0.230	0.248	92,754	100,881	51	39
104	0.284	0.277	99,207	103,413	22	39
109	0.278	0.280	77,716	85,363	214	8
111	0.198	0.237	65,225	74,669	13	1
113	0.239	0.291	82,564	80,993	174	6
114	0.260	0.280	96,101	109,053	64	26
118	0.274	0.254	101,712	106,606	59	24
Average	0.254	0.270	87,098	92,919	85	19
SD	±0.02	±0.02	±12,487	±13,442	±72	±15

Unlike total axon number, the ratio of cross-sectional area was more variable between animals (Table 1; Fig. 7B). Although there was a trend toward shrinkage of the treated nerves (indicated by ratios <1), this trend was not statistically significant ($P = 0.1$; Fig. 7B). These data suggest that the overall area of the optic nerve did not accompany the modest axon loss observed with intermittent IOP elevation. However, the trend toward smaller nerves in the treated eyes suggested that gross changes in optic nerve morphology may evolve in this model.

Intermittent IOP Elevation Induces Glial Reactivity

In addition to changes in axon morphology, pathology in the optic nerve is often accompanied by changes in glial cell populations. Besides oligodendrocytes, astrocytes are the primary glial cell in the optic nerve and are located in the interfascicular space. In response to noxious stimuli, astrocytes become reactive, which includes hypertrophic changes in morphology and upregulation of GFAP.[46–50]

To evaluate the reactivity state of astrocytes, spectral analysis of GFAP immunolabeling was performed in the untreated and treated optic nerves of six animals (Fig. 8). Across all nerves examined, the average signal intensity of GFAP labeling increased by 36% in treated nerves compared with untreated nerves (Figs. 8A–C; $P = 0.03$). Although GFAP intensity increased in all treated nerves, there was interanimal variability in the magnitude of this increase. Fold increases in GFAP intensity in individual nerves ranged from 1.05 to 1.69 (Fig. 8C). These data suggest that intermittent elevations in IOP are accompanied by increased reactivity of astrocytes that, though variable in its magnitude, includes increased GFAP expression.

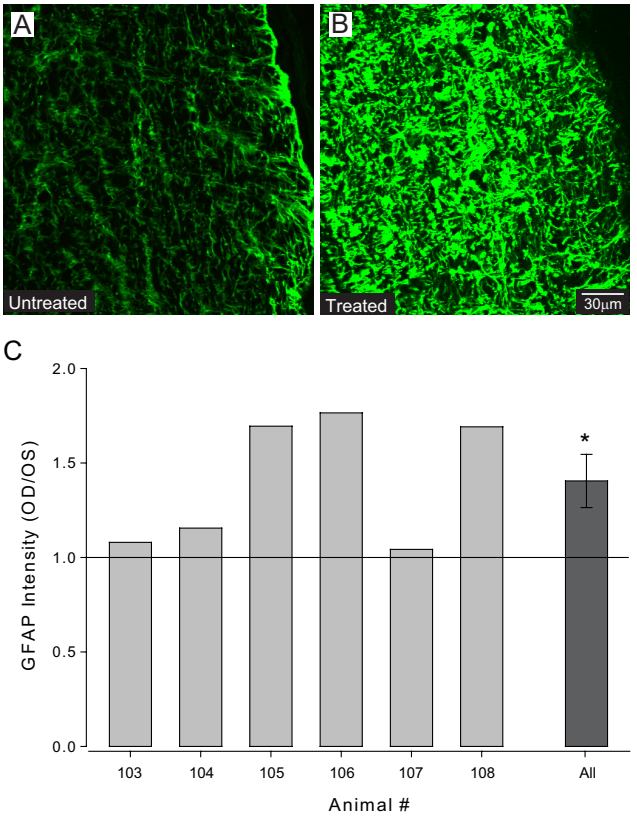

FIGURE 8. (**A**, **B**) Representative semiquantitative confocal micrographs from animal 106 of longitudinal optic nerve sections immunohistochemically labeled for GFAP (*green*). Treated optic nerves (**B**) subjectively demonstrate greater intensity of GFAP labeling than untreated optic nerves (**A**). (**C**) Spectral analysis of GFAP signal intensity represented as the ratio of signal intensity in treated versus untreated optic nerves. Graph depicts the ratios for individual animals (*light gray*) and the combined ratio across all animals (*dark gray*). On average, the intensity of GFAP labeling was 36% greater in treated optic nerves compared with untreated nerves ($P = 0.03$). *Asterisk*: statistical significance.

DISCUSSION

The presented model provides an opportunity to investigate the effects of intermittent elevation of IOP on the rat eye. Targeted IOP elevations are possible with the adjustable ligature. It may be easily tightened or loosened to achieve the desired IOP. Daily IOP elevations for 1 hour are possible with topical anesthesia in this animal model without systemic stress at least up to 6 weeks. This is an advantage over the confounding variables of systemic anesthesia and surgical manipulation to raise IOP when it is desired to evaluate the earliest effects of elevated IOP. Others have clearly documented the detrimental effects such as weight loss with frequent systemic anesthesia administration to measure the IOP in rats.[51] As can be seen in Figure 3, the effect of the lasso was substantial for the IOP in the treated eye, whereas the untreated eye underwent statistical but little clinically relevant change in IOP. This elevation was sustainable over the 1-hour treatment period with only a slight decrement.

Unlike the genetic model of the DBA/2J mouse,[25] the angles in the proposed model appear to remain open without synechiae. The development of synechiae would be expected to produce chronic elevations of IOP. That IOP returned to baseline levels even at the end of the 6-week trial further supports the lack of synechiae in this model. Unlike other models,[22,25,29] inflammation was not noted in the anterior chamber (Fig. 4). Histologic examination of retinal sections also revealed that the retinal layers remained intact (Fig. 4). This is in contrast to that observed after acute ischemia-reperfusion manipulations in which the IOP is elevated above perfusion pressure for only 1 hour and is followed over time.[34] Overall, our data suggest that the vascular loop elevates IOP without significant ischemic damage.

The shortest period of moderate IOP elevation required to produce degenerative changes in the retina and optic nerve is unknown. Here we describe various indicators of degeneration in the ganglion cell and nerve fiber layers of the retina and optic nerve after only 1 hour of elevated IOP daily for 6 weeks. In the retina, we demonstrated that intermittent IOP elevation to 35 mm Hg induced both a reduction in NFL thickness and a decrease in the number of cell soma in the ganglion cell layer that, though present, is lower than that reported in an advanced glaucoma model (Fig. 5).[52] Intermittent IOP elevations had a greater impact on NFL thickness (22%–25%) than the number of cell soma in the ganglion cell layer (7%–10%). This is likely because of the presence of displaced amacrine cells, whose processes are not a component of the NFL, in the ganglion cell layer.

Our qualitative analysis of optic nerve by both light and electron microscopy revealed an increase in the number of degenerative axon profiles and vacuolization in the extra-axonal space (Fig. 6). At the level of individual axons, we demonstrated evidence of disorganized myelin sheaths, disruption of neurofilaments, and enlargement of the axoplasmic space (Fig. 6). These axonal changes are consistent with optic nerve axon degeneration well described in other studies.[21,25,30,53–55] Interestingly, our quantitative analysis of degenerative axon profiles revealed significant variability among treated eyes despite almost identical IOP elevation. Although it is possible that

the small variation in age (2 months) among our subjects could contribute to variability between individuals, it is also possible that these differences represent intrinsic variability that is dependent on a variety of factors, including genetic differences. It is intriguing that the highly uniform nature of IOP elevation in this model may provide a means to investigate responses to elevated IOP at the level of the individual. It is important to note that though there was individual variability in the number of degenerative profiles among treated eyes, all treated eyes qualitatively demonstrated some indicators of degeneration (e.g., increase in axoplasmic space, disruption of neurofilaments) compared with their contralateral untreated eye. In any biological system, including the optic nerve, the rate and features of the degenerative process are not uniform across cells exposed to the same stimulus. This is well demonstrated in vitro, when exposure to elevated hydrostatic pressure is identical for all cells on the culture plate but induces apoptosis in RGCs that increases over time rather than occurring all at once.[56]

In accordance with our retinal analyses, quantitative analysis of total axon number revealed a decrease of 6% in optic nerves from treated eyes versus the contralateral untreated eye (Table 1; Fig. 7). This decrease in axon number appeared to be diffuse rather than focal across the optic nerve. Over longer periods of exposure, this diffuse degeneration could remain diffuse over time,[40] evolve into primarily focal axonal lesions,[19] or evolve into a combination of diffuse to focal defects.[57]

Published reports of axon counts in rat optic nerve vary depending on several factors, including age extremes of the rat[42,58,59] and the sampling techniques used.[23,42,58–60] Our average of 92,919 ± 13,442 axons per untreated nerve compares favorably with the approximate 96,200 to 108,100 axons in albino rats, as described by time-intensive transmission electron microscopy sampling techniques.[58,60] Cepurna et al.[42] found more axons (117,900 ± 11,000) in the Brown Norway optic nerve with electron microscopy. Although the smallest axons may be missed in quantitative whole nerve counts at the light microscopic level, their presence or absence would also be overlooked in the alternative qualitative grading systems.[32,61] Furthermore, when performing axon counts, it must be considered that there is biological variability among animals and between eyes in the same animal. Cepurna et al.[42] reported up to 8.5% variability of optic nerve axon counts between the right and left eye of an animal with a much greater variability among eyes of different 5-month-old Brown Norway rats.[42] To compensate for the variability among animals, axon counts were evaluated as treated/untreated ratio for each animal. In support of our findings in the optic nerve, the magnitude of axon loss we detected (6%) 2.5 mm from the globe was strikingly similar to that of cell soma loss in the ganglion cell layer (7%–10%).

In our quantitative analyses of optic nerve, we also discovered a tendency toward shrinkage of the optic nerve. However, this trend was not significant (Fig. 7). It is possible that this tendency for smaller optic nerves in treated eyes could result from a loss of axons and, therefore, an increase in severity over time. We cannot rule out the possibility that this trend could also be attributed to histologic shrinkage of the tissue. This is particularly true given the variability across animals.

In addition to our analysis of RGC degeneration, we also examined the impact of intermittent IOP elevations on the reactivity of astrocytes in the optic nerve. In central nervous system injury and human glaucoma, hypertrophy and upregulation of GFAP in astrocytes are components of the glial cell response to neurodegeneration.[46–50] For animal glaucoma models with continuous elevations of IOP, the timeline of astrocyte reactivity varies.[21,62–64] In advanced glaucomatous damage, elevated GFAP was prevalent in the optic nerves in animal models.[63,64] The effect of intermittent IOP on glial cell reactivity has not been examined previously. In this model, the upregulation of GFAP was evident in optic nerves from treated eyes compared with the contralateral untreated eyes (Fig. 8). As in our analysis of degenerative profiles in the optic nerve, there was significant variability among treated eyes. Interestingly, the magnitude of GFAP reactivity correlated with the number of degenerative profiles; the two animals (103 and 104) with the smallest ratios of degenerative profiles also had modest increases in GFAP intensity (compare Fig. 6 and Fig. 8). Furthermore, these two animals had total axon counts that were close to the mean for treated eyes. These data suggest that though the irreversible outcome of the disease process (i.e., axon loss) was similar among treated animals, the process by which this outcome is achieved may vary inherently between individuals with nearly identical insults.

In summary, consistent intermittent IOP elevations can be produced daily for 1 hour in the adult rat without evidence of overt ischemia or stress to the animal. Six weeks of daily moderate IOP elevations will produce early histologic glaucomatous damage with modest degeneration of RGCs and their axons that share characteristics with degeneration induced by continual elevations of IOP. This model provides an opportunity with which to evaluate early molecular and histologic responses to IOP fluctuations that are increasingly believed to contribute to glaucomatous progression in a controlled and reproducible manner. In addition, our data suggest that the highly controlled nature of these IOP elevations provides the potential to examine individual variability in the IOP-induced degenerative process without confounding factors, such as rate and magnitude of IOP elevation. This knowledge may assist in developing therapies to effectively treat injured retinal ganglion cells and their axons in an environment of fluctuating IOP.

Acknowledgments

The authors thank Peter Haddix, Anta'Sha Jones, Lauren Knish, Ratna Prasad, Meena Putatunda, Richard Robinson, Sanaz Saadat, Stephanie Sims, and Guangming Wu for valuable technical assistance; David Calkins for algorithms for the optic nerve analysis; and the staff of the Cell Imaging Core at Vanderbilt University Medical Center for aid in obtaining micrographs.

References

1. Konstas AG, Maskaleris G, Gratsonidis S, Sardelli C. Compliance and viewpoint of glaucoma patients in Greece. *Eye.* 2000;14(5):752–756.
2. Sleath B, Robin AL, Covert D, Byrd JE, Tudor G, Svarstad B. Patient-reported behavior and problems in using glaucoma medications. *Ophthalmology.* 2006;113(3):431–436.
3. Henderer JD, Wilson RP, Moster MR, et al. Timolol/dorzolamide combination therapy as initial treatment for intraocular pressure over 30 mm Hg. *J Glaucoma.* 2005;14(4):267–270.
4. Carlson KH, McLaren JW, Topper JE, Brubaker RF. Effect of body position on intraocular pressure and aqueous flow. *Invest Ophthalmol Vis Sci.* 1987;28(8):1346–1352.
5. Weinreb RN, Cook J, Friberg TR. Effect of inverted body position on intraocular pressure. *Am J Ophthalmol.* 1984;98(6):784–787.
6. Drance SM. The significance of the diurnal tension variations in normal and glaucomatous eyes. *Arch Ophthalmol.* 1960;64:494–501.
7. Liu JH, Zhang X, Kripke DF, Weinreb RN. Twenty-four-hour intraocular pressure pattern associated with early glaucomatous changes. *Invest Ophthalmol Vis Sci.* 2003;44(4):1586–1590.
8. Mosaed S, Liu JH, Weinreb RN. Correlation between office and peak nocturnal intraocular pressures in healthy subjects and glaucoma patients. *Am J Ophthalmol.* 2005;139(2):320–324.

9. Hara T, Hara T, Tsuru T. Increase of peak intraocular pressure during sleep in reproduced diurnal changes by posture. *Arch Ophthalmol.* 2006;124(2):165–168.
10. Zeimer RC, Wilensky JT, Gieser DK, Viana MA. Association between intraocular pressure peaks and progression of visual field loss. *Ophthalmology.* 1991;98(1):64–69.
11. Hughes E, Spry P, Diamond J. 24-Hour monitoring of intraocular pressure in glaucoma management: a retrospective review. *J Glaucoma.* 2003;12(3):232–236.
12. Sung VC, Barton K. Management of inflammatory glaucomas. *Curr Opin Ophthalmol.* 2004;15(2):136–140.
13. Bui CM, Chen H, Shyr Y, Joos KM. Discontinuing nasal steroids might lower intraocular pressure in glaucoma. *J Allergy Clin Immunol.* 2005;116(5):1042–1047.
14. Kitazawa Y, Horie T. Diurnal variation of intraocular pressure in primary open-angle glaucoma. *Am J Ophthalmol.* 1975;79(4):557–566.
15. Konstas AG, Topouzis F, Leliopoulou O, et al. 24-hour intraocular pressure control with maximum medical therapy compared with surgery in patients with advanced open-angle glaucoma. *Ophthalmology.* 2006;113(5):761–765.
16. Bergea B, Bodin L, Svedbergh B. Impact of intraocular pressure regulation on visual fields in open-angle glaucoma. *Ophthalmology.* 1999;106(5):997–1004.
17. Nouri-Mahdavi K, Hoffman D, Coleman AL, et al. Advanced Glaucoma Intervention Study: predictive factors for glaucomatous visual field progression in the Advanced Glaucoma Intervention Study. *Ophthalmology.* 2004;111(9):1627–1623.
18. Shareef SR, Garcia-Valenzuela E, Salierno A, Walsh J, Sharma SC. Chronic ocular hypertension following episcleral venous occlusion in rats. *Exp Eye Res.* 1995;61(3):379–382.
19. Morrison JC, Moore CG, Deppmeier LMH, Gold BG, Meshul CK, Johnson EC. A rat model of chronic pressure-induced optic nerve damage. *Exp Eye Res.* 1997;64(1):85–96.
20. John SW, Smith RS, Savinova OV, et al. Essential iris atrophy, pigment dispersion, and glaucoma in DBA/2J mice. *Invest Ophthalmol Vis Sci.* 1998;39(6):951–962.
21. Johnson EC, Deppmeier LM, Wentzien SK, Hsu I, Morrison JC. Chronology of optic nerve head and retinal responses to elevated intraocular pressure. *Invest Ophthalmol Vis Sci.* 2000;41(2):431–442.
22. Goldblum D, Mittag T. Prospects for relevant glaucoma models with retinal ganglion cell damage in the rodent eye. *Vision Res.* 2002;42(4):471–478.
23. Levkovitch-Verbin H, Quigley HA, Martin KR, Valenta D, Baumrind LA, Pease ME. Translimbal laser photocoagulation to the trabecular meshwork as a model of glaucoma in rats. *Invest Ophthalmol Vis Sci.* 2002;43(2):402–410.
24. Morrison JC. Elevated intraocular pressure and optic nerve injury models in the rat. *J Glaucoma.* 2005;14(4):315–317.
25. Inman DM, Sappington RM, Horner PJ, Calkins DJ. Quantitative correlation of optic nerve pathology with ocular pressure and corneal thickness in the DBA/2 mouse model of glaucoma. *Invest Ophthalmol Vis Sci.* 2006;47(3):986–996.
26. Naskar R, Thanos S. Retinal gene profiling in a hereditary rodent model of elevated intraocular pressure. *Mol Vis.* 2006;12:1199–1210.
27. Schlamp CL, Li Y, Dietz JA, Janssen KT, Nickells RW. Progressive ganglion cell loss and optic nerve degeneration in DBA/2J mice is variable and asymmetric. *BMC Neurosci.* 2006;7:66.
28. Pang IH, Clark AF. Rodent models for glaucoma retinopathy and optic neuropathy. *J Glaucoma.* 2007;16(5):483–505.
29. Nissirios N, Chanis R, Johnson E, et al. Comparison of anterior segment structures in two rat glaucoma models: an ultrasound biomicroscopic study. *Invest Ophthalmol Vis Sci.* 2008;49(6):2478–2482.
30. Buckingham BP, Inman DM, Lambert W, et al. Progressive ganglion cell degeneration precedes neuronal loss in a mouse model of glaucoma. *J Neurosci.* 2008;28(11):2735–2744.
31. McKinnon SJ, Schlamp CL, Nickells RW. Mouse models of retinal ganglion cell death and glaucoma. *Exp Eye Res.* 2009;88(4):816–824.
32. Jia L, Cepurna WO, Johnson EC, Morrison JC. Patterns of intraocular pressure elevation after aqueous humor outflow obstruction in rats. *Invest Ophthalmol Vis Sci.* 2000;41(6):1380–1385.
33. Foulds WS, Johnson NF. Rabbit electroretinogram during recovery from induced ischemia. *Trans Ophthalmol Soc UK.* 1974;94(2):383–393.
34. Selles-Navarro I, Villegas-Perez MP, Salvador-Silva M, Ruiz-Gomez JM, Vidal-Sanz M. Retinal ganglion cell death after different transient periods of pressure-induced ischemia and survival intervals. *Invest Ophthalmol Vis Sci.* 1996;37(10):2002–2014.
35. Bui BV, Edmunds B, Cioffi GA, Fortune B. The gradient of retinal functional changes during acute intraocular pressure elevation. *Invest Ophthalmol Vis Sci.* 2005;46(1):202–213.
36. Morrison JC, Johnson EC, Cepurna W, Jia L. Understanding mechanisms of pressure-induced optic nerve damage. *Prog Retin Eye Res.* 2005;24(2):217–240.
37. Laquis S, Chaudhary P, Sharma SC. The patterns of retinal ganglion cell death in hypertensive eyes. *Brain Res.* 1998;784(1):100–104.
38. Kawaguchi I, Higashide T, Ohkubo S, et al. In vivo imaging and quantitative evaluation of the rat retinal nerve fiber layer using scanning laser ophthalmoscopy. *Invest Ophthalmol Vis Sci.* 2006;47:2911–2916.
39. Zhang X, Chintala SK. Influence of interleukin-1 beta induction and mitogen-activated protein kinase phosphorylation on optic nerve ligation-induced matrix metalloproteinase-9 activation in the retina. *Exp Eye Res.* 2004;78:849–860.
40. Sappington RM, Carlson BJ, Crish SD, Calkins DJ. The microbead occlusion model: a paradigm for induced ocular hypertension in rats and mice. *Invest Ophthalmol Vis Sci.* 2010;51(1):207–216.
41. Baltan S, Inman DM, Danilov CA, Morrison RS, Calkins DJ, Horner PJ. Metabolic vulnerability disposes retinal ganglion cell axons to dysfunction in a model of glaucomatous degeneration. *J Neurosci.* 2010;30(16):5644–5652.
42. Cepurna WO, Kayton RJ, Johnson EC, Morrison JC. Age related optic nerve axonal loss in adult Brown Norway rats. *Exp Eye Res.* 2005;80(6):877–884.
43. Jonas JB, Schmidt AM, Müller-Bergh JA, Naumann GO. Optic nerve fiber count and diameter of the retrobulbar optic nerve in normal and glaucomatous eyes. *Graefes Arch Clin Exp Ophthalmol.* 1995;233(7):421–424.
44. Mabuchi F, Aihara M, Mackey MR, Lindsey JD, Weinreb RN. Optic nerve damage in experimental mouse ocular hypertension. *Invest Ophthalmol Vis Sci.* 2003;44(10):4321–4330.
45. Ito Y, Shimazawa M, Chen YN, et al. Morphological changes in the visual pathway induced by experimental glaucoma in Japanese monkeys. *Exp Eye Res.* 2009;89(2):246–255.
46. Vanezis P, Chan KK, Scholtz CL. White matter damage following acute head injury. *Forensic Sci Int.* 1987;35(1):1–10.
47. Takamiya Y, Kohsaka S, Toya S, Otani M, Tsukada Y. Immunohistochemical studies on the proliferation of reactive astrocytes and the expression of cytoskeletal proteins following brain injury in rats. *Brain Res.* 1988;466(2):201–210.
48. Hatten ME, Liem RK, Shelanski ML, Mason CA. Astroglia in CNS injury. *Glia.* 1991;4(2):233–243.
49. Varela HJ, Hernandez MR. Astrocyte responses in human optic nerve head with primary open-angle glaucoma. *J Glaucoma.* 1997;6(5):303–313.
50. Joos KM, Mawn LA, Shen JH, Casagrande VA. Chronic and acute analysis of optic nerve sheath fenestration with the free electron laser in monkeys. *Lasers Surg Med.* 2003;32(1):32–41.
51. Jia L, Cepurna WO, Johnson EC, Morrison JC. Effect of general anesthetics on IOP in rats with experimental aqueous outflow obstruction. *Invest Ophthalmol Vis Sci.* 2000;41(11):3415–3419.
52. Ueda J, Sawaguchi S, Hanyu T, et al. Experimental glaucoma model in the rat induced by laser trabecular photocoagulation after an intracameral injection of India ink. *Jpn J Ophthalmol.* 1998;42(5):337–344.
53. Pease ME, McKinnon SJ, Quigley HA, Kerrigan-Baumrind LA, Zack DJ. Obstructed axonal transport of BDNF and its receptor TrkB in experimental glaucoma. *Invest Ophthalmol Vis Sci.* 2000;41(3):764–774.
54. Saggu SK, Chotaliya HP, Cai Z, Blumbergs P, Casson RJ. The spatiotemporal pattern of soma and axonal pathology after

perikaryal excitotoxic injury to retinal ganglion cells: a histological and morphometric study. *Exp Neurol.* 2008;211(1):52–58.

55. Crish SD, Sappington RM, Inman DM, Horner PJ, Calkins DJ. Distal axonopathy with structural persistence in glaucomatous neurodegeneration. *Proc Natl Acad Sci U S A.* 2010;107(11):5196–5201.
56. Sappington RM, Chan M, Calkins DJ. Interleukin-6 protects retinal ganglion cells from pressure-induced death. *Invest Ophthalmol Vis Sci.* 2006;47(7):2932–2942.
57. Schlamp CL, Li Y, Dietz JA, Janssen KT, Nickells RW. Progressive ganglion cell loss and optic nerve degeneration in DBA/2J mice is variable and progressive. *BMC Neurosci.* 2006;7:66.
58. Hunter A, Bedi KS. A quantitative morphological study of interstrain variation in the developing rat optic nerve. *J Comp Neurol.* 1986;245(2):160–166.
59. Ricci A, Bronzetti E, Amenta F. Effect of ageing on the nerve fibre population of rat optic nerve. *Gerontology.* 1988;34(5–6):231–235.
60. Sugimoto T, Fukuda Y, Wakakuwa K. Quantitative analysis of a cross-sectional area of the optic nerve: a comparison between albino and pigmented rats. *Exp Brain Res.* 1984;54(2):266–274.
61. Chauhan BC, LeVatte TL, Garnier KL, et al. Semiquantitative optic nerve grading scheme for determining axonal loss in experimental optic neuropathy. *Invest Ophthalmol Vis Sci.* 2006;47(2):634–640.
62. Lam TT, Kwong JM, Tso MO. Early glial responses after acute elevated intraocular pressure in rats. *Invest Ophthalmol Vis Sci.* 2003;44(2):638–645.
63. Hernandez MR. The optic nerve head in glaucoma: role of astrocytes in tissue remodeling. *Prog Retin Eye Res.* 2000;19(3):297–321.
64. Furuyoshi N, Furuyoshi M, May CA, Hayreh SS, Alm A, Lutjen-Drecoll E. Vascular and glial changes in the retrolaminar optic nerve in glaucomatous monkey eyes. *Ophthalmologica.* 2000;214(1):24–32.